Divalent Cations Stimulate Preferential Recognition of a Viral DNA End by HIV-1 Integrase†

Jizu Yi, Ernest Asante-Appiah,‡ and Anna Marie Skalka*

Institute for Cancer Research, Fox Chase Cancer Center, 7701 Burholme Avenue, Philadelphia, Pennsylvania 19111

Received December 4, 1998; Revised Manuscript Received April 19, 1999

ABSTRACT: In the presence of a divalent metal cofactor (Mg^{2+} or Mn^{2+}), retroviral-encoded integrase (IN) catalyzes two distinct reactions: site-specific cleavage of two nucleotides from both 3′ ends of viral DNA, and sequence-independent joining of the recessed viral ends to staggered phosphates in a target DNA. Here we investigate human immunodeficiency virus type 1 (HIV-1) IN−DNA interactions using surface plasmon resonance. The results show that IN forms tight complexes both with duplex oligonucleotides that represent the viral DNA ends and with duplex oligonucleotides with an unrelated sequence that represent a target DNA substrate. The IN−DNA complexes are stable in 4.0 M NaCl, or 50% (v/v) methanol, but they are not resistant to low concentrations of SDS, indicating that their stability is highly dependent on structural features of the protein. Divalent metal cofactors exert two distinct effects on the IN−DNA interaction. Mn^{2+} inhibits IN binding to a model target DNA with the apparent K_d increasing approximately 3-fold in the presence of this cation. On the other hand, Mn^{2+} (or Mg^{2+}) stimulates the binding of IN to a model viral DNA end, decreasing the apparent K_d of this IN−viral DNA complex approximately 6-fold. Such metal-mediated stimulation of the binding of IN to the viral DNA is totally abolished by substitution of the subterminal conserved CA/GT bp with a GT/CA bp, and is greatly diminished when the viral DNA end is recessed or "pre-processed." IN binds to a viral duplex oligonucleotide whose end was extended with nonviral sequences with kinetics similar to the nonviral model target DNA. This suggests that IN can distinguish the integrated DNA product from the viral donor DNA in the presence of divalent metal ion. Thus, our results show that preferential recognition of viral DNA by HIV-1 IN is achieved only in the presence of metal cofactor, and requires a free, wild-type viral DNA end.

Integration of double-stranded viral DNA into the chromosome of host cells is an essential step in the life cycle of retroviruses, including human immunodeficiency virus type 1 (HIV-1)[1] (*1*). The integration reaction is catalyzed by the virally encoded enzyme integrase (IN). The reaction proceeds in two discrete steps: first, removal of dinucleotides from both 3′ ends of the viral DNA adjacent to a conserved 5′-CA-3′ dinucleotide; second, coordinated covalent joining of the 3′-oxygen of the recessed viral DNA ends to staggered 5′-phosphate groups in target chromosomal DNA in the host cells (*2*, *3*). Retroviral integrase proteins have three distinct domains that have been characterized both structurally and functionally (*4*). The N-terminal domain of HIV-1 IN comprises approximately the first 49 amino acids. The catalytic core domain spans a region from residue 50 to residue 212, and the C-terminal domain from residue 220 to residue 270, plus a tail comprising residues 271−288 (Figure 1A). The N-terminal domain is characterized by a highly conserved HHCC motif which binds a zinc ion (*5*, *6*). Binding of Zn^{2+} stabilizes the structure of the HIV-1 IN N-terminal domain (*7*, *8*), and stimulates the Mg^{2+}-dependent activity in vitro, possibly by enhancement of IN multimerization (*8*−*10*). The catalytic core domain, containing the active site of IN, includes a highly conserved D,D(35)E motif. This motif was proposed to contribute to the binding of the metal cofactors, Mn^{2+} or Mg^{2+} (*11*, *12*), and this proposal has been verified by analysis of X-ray cocrystal structures of the ASV IN core domain complexed with divalent cations such as Mn^{2+}, Mg^{2+}, Zn^{2+}, Ca^{2+}, and Cd^{2+} (*13*, *14*), and of the HIV-1 IN core domain with Mg^{2+} (*15*, *16*). The C-terminal region is the least conserved among retroviral integrases. It functions as a nonspecific DNA binding domain, independent of the presence of divalent cations (*17*−*19*).

During integration, IN proteins must recognize and bind to both the viral DNA and target DNA substrates. Extensive biochemical and genetic studies have demonstrated substrate

† This work was supported by NIH Grants CA71515 and AI40385 and Institutional Grant CA06927 from the National Institutes of Health, and also by an appropriation from the Commonwealth of Pennsylvania. The contents of this manuscript are solely the responsibility of the authors and do not necessarily represent the official views of the National Cancer Institute, or any other sponsoring organization.

* To whom correspondence should be addressed. Fax: 215-728-2778. Telephone: 215-728-2490.

‡ Present address: Department of Biochemistry and Molecular Biology, Merck Frosst Center for Therapeutic Research, P.O. Box 1005, Pointe-Claire-Dorval, Quebec H9R 4P8, Canada.

[1] Abbreviations: HIV-1, human immunodeficiency virus type 1; IN, integrase; SPR, surface plasmon resonance; NHS, *N*-hydroxysuccinimide; EDC, *N*-ethyl-*N*′-(3-diethylaminopropyl)carbodiimide; HBS, Hepes-buffered saline; IN-3CS, integrase with substitutions of three cysteine residues (C56, C65, C280) with serines; DTT, dithiothreitol; RU, relative response/resonance unit; MLV, Moloney murine leukemia virus; LTR, long terminal repeat; RSV, Rous sarcoma virus.

10.1021/bi982870n CCC: $18.00
Published on Web 06/10/1999

specificity of retroviral INs for their cognate DNA ends (*20*−*32*). It was also shown that HIV-1 IN forms stable complexes with viral DNA substrates (*33*, *34*). The assembly of these complexes requires both full-length IN and the presence of divalent cations, such as the metal cofactors Mn^{2+} or Mg^{2+}. The complexes are resistant to competition by nonviral DNA, to washing with relatively high concentrations of salt, and to exonuclease digestion (*33*−*37*). Nevertheless, HIV-1 IN appears to exhibit a very limited substrate binding specificity. The binding affinity of the protein to a target DNA substrate was estimated to be nearly the same as to the viral donor DNA substrate (*36*, *38*). Previous investigations of HIV-1 IN−DNA interactions by mobility shift assay (*38*, *39*), UV-induced cross-linking (*36*, *40*, *41*), Southwestern blot (*17*, *18*), and filter binding assay (*42*) were focused either on the ability of the protein to bind to viral DNA substrates or on qualitative analysis of the IN−DNA interaction. None of the methods used to date has been able to distinguish quantitatively between the binding of HIV-1 IN to the viral DNA substrate and binding to a nonviral target DNA substrate. The relative effects of divalent cation cofactors on the interaction of IN with these two DNA substrates were also not quantified.

In this study, we employed surface plasmon resonance (SPR) to investigate the binding of HIV-1 IN to DNA substrates immobilized on the surface of a biosensor chip. SPR, with the measurement of real-time interactions, allows us to monitor directly the formation and decomposition of macromolecular complexes under different conditions (*43*). These real-time kinetic measurements provide accurate rate constants for dissociation and association of the macromolecular interactions (*44*). It was found that HIV-1 IN forms stable complexes with both viral donor DNA and nonviral target DNA in the presence or in the absence of divalent cations. However, Mn^{2+} or Mg^{2+} stimulates the binding of IN to the model viral DNA substrate, but reduces binding to a model target DNA substrate. The effect of divalent cations on the DNA binding activity of IN suggests that the metal ion cofactor promotes the ability of IN to recognize viral DNA preferentially, and that four base pairs at the free viral DNA ends are especially important for such recognition.

EXPERIMENTAL PROCEDURES

Materials. Streptavidin and biotin were purchased from Pierce. Primary amine chemical coupling kit containing *N*-hydroxysuccinimide (NHS), *N*-ethyl-*N*′-(3-diethylaminopropyl)carbodiimide (EDC), and 1.0 M ethanolamine/hydrochloride (pH 8.0), research grade sensor CM-5 or SA chips, Hepes-buffered saline (HBS) [10 mM HEPES, pH 7.5, 150 mM NaCl, 3.4 mM EDTA, 0.005% (v/v) surfactant P20], and surfactant P20 were from Pharmacia. Other chemicals were from Fisher Scientific. All oligonucleotides were synthesized on an ABI DNA synthesizer in the Fox Chase Cancer Center DNA Synthesis Facility, purified by electrophoresis in denaturing gels (20% polyacrylamide gels containing 7 M urea), and electroeluted from gel slices with a Centrolutor (Amicon).

Construction of the HIV-1 IN-3CS Expression Plasmid. Construction of plasmid pET29b HIV-1 IN has been reported (*45*). The single substitution mutant pET29b HIV-1 IN C280S was constructed by established methods (*46*). The oligonucleotide that was used for the mutagenesis included the recognition site for the restriction enzyme *Asp*I which was used for diagnosis of positive clones. The introduction of the C280S-encoding mutation was confirmed by DNA sequencing. Single-stranded DNA was subsequently isolated from pET29b HIV-1 IN C280S (*46*) and used as template for the construction of the double substitution mutants pET29b HIV-1 IN C56S, C280S; pET29b HIV-1 IN C65S, C280S; and pET29b HIV-1 IN C130S, C280S (Figure 1A). The oligonucleotide that was used for introduction of the C56S substitution ensured the elimination of the unique restriction site for *Sal*I in positive clones. A restriction site for *Pvu*II was removed while an *Nhe*I site was introduced in the construction of the mutants encoding C65S and C130S, respectively. The successful construction of the double mutants was also confirmed by sequencing the putative positive clones. A clone encoding the triple substitution pET29b HIV-1 IN C56S, C65S, C280S (HIV-1 IN-3CS) was constructed by introducing a C56S-encoding mutation into the C65S, C280S double mutant by site-directed mutagenesis. Positive clones of the pET29b HIV-1 IN-3CS construct were further sequenced to confirm the substitution of all three cysteine codons and the integrity of the clone.

Following the successful construction of the single, double, and triple mutants, DNAs from positive clones were introduced into competent *E. coli* BL21(DE3) cells by transformation to check for protein expression and, subsequently, to purify the HIV-1 IN derivatives. The solubilities of the purified proteins were then assessed. In contrast to wild-type HIV-1 IN which is soluble to about 1 mg/mL, the singly substituted mutant, HIV-1 IN C280S, is soluble up to approximately 3 mg/mL and IN-3CS to approximately 15 mg/mL. However, substitution of serine residues for all four cysteine residues outside of the HHCC domain (i.e., including C130) results in a protein that is less soluble (<1 mg/mL) than the wild-type protein.

Purification of Wild-Type HIV-1 Integrase and Mutants. Wild-type HIV-1 IN and derivatives were purified as described previously (*47*) with minor modifications. Cells were lysed by two passes through a French pressure cell at 18 000 psi in a buffer containing 20 mM HEPES, pH 7.5, 5 mM imidazole, and 2 M KCl. The cell lysate was then subjected to centrifugation at 31000*g* for 30 min. The salt concentration of the supernatant was adjusted to 1 M KCl, and then it was applied to a nickel-charged HiTrap-Chelating column (Pharmacia). The column was washed with 10 column volumes of binding buffer (20 mM HEPES, pH 7.5, 1 M KCl, 5 mM imidazole), and the protein was eluted using a linear gradient of imidazole (5 mM−1 M) in 10 column volumes. Fractions containing the protein were pooled and subsequently passed over a HiTrap-heparin column (Pharmacia) equilibrated in 20 mM HEPES, 250 mM KCl, 0.1 mM EDTA, 1 mM dithiothreitol (DTT), pH 7.5. After the column was washed with 10 column volumes of binding buffer, the protein was eluted with a linear gradient of 250 mM−1 M KCl in the above HEPES buffer. A final hydrophobic interaction chromatography step on methacrylate beads yielded homogeneous preparations that were stored in 20 mM HEPES, pH 7.5, 1 mM DTT, 500 mM KCl, and 40% (v/v) glycerol at −20 °C. All purification steps were carried out at 4 °C or on ice.

Oligonucleotide Activity Assay. Activity of the HIV-1 IN derivatives was assayed as reported previously (*45*).

Oligonucleotide Substrates. The sequences of viral DNA substrates were matched to the U5 end of HIV-1 viral DNA. The model target DNA substrates have no sequences that match with viral DNA ends. Biotin was incorporated at either the 5′ end of the viral DNA positive strand or the 3′ end of the negative strand for immobilization of oligonucleotides on the surface of a biosensor chip. The following oligonucleotide substrates, in which the conserved CA/GT base components or mutants thereof are underlined, were used as HIV-1 IN substrates in this study:

(1) 21 bp viral DNA end substrate (U5 end): top strand (AS 995), 5′-GTGTGGAAAATCTCTAG*CA*GT-3′; bottom strand (AS 997), biotin-3′-GCACACCTTTTAGAGATC*GT*-CA-5′

(2) Preprocessed/recessed viral DNA end (donor DNA substrate for the joining reaction of integration): top strand (AS 736), 5′-GTGTGGAAAATCTCTAG*CA*-3′; bottom strand, the same as AS 997

(3) 21 bp mutated viral DNA end substrate: top strand (AS 833), 5′-GTGTGGAAAATCTCTAG*GT*GT-3′; bottom strand (AS 1080), biotin-3′-GCACACCTTTTAGAGATC-*CA*CA-5′

(4) 35 bp comprising the viral end sequence blocked by an extension of 14 bp of nonviral sequence: top strand (AS 1037), 5′-GTGTGGAAAATCTCTAG*CA*GTGGCTGCAG-GTCGAC-3′; bottom strand (AS1038), biotin-3′-CACAC-CTTTTAGAGATC*GT*CACCGACGTCCAGCTG-5′

(5) 24 bp model target DNA substrate: top strand (AS 1032), biotin-5′-CTACCGCATTAAAGCTTATCGCGG-3′; bottom strand (AS 798), 3′-GATGGCGTAATTTCGAAT-AGCGCC-5′

(6) 40 bp model target substrate: top strand (AS 1033), biotin-5′-CCCGGTTTGGAAAGGCCCTGCTGCT-CTCCTGTGGAAGGGT-3′; bottom strand (AS 949), 3′-GGGCCAAACCTTTCCGGGACGACGAGAG-GACACCTTCCCA-5′

In oligonucleotides AS 997 and AS 1080, an extra G residue was included adjacent to the biotin to reduce possible steric hindrance by streptavidin upon annealing of double-stranded oligonucleotides on the chip surface.

Immobilization of DNA on a Sensor Chip. BIAcore experiments were performed on a BIAcore 1000 instrument (Fannie E. Ripple Biotechnology Facility, Fox Chase Cancer Center, Philadelphia, PA). Immobilization of oligonucleotides was through biotin−streptavidin interaction as described by Bonderson et al. (*48*). Streptavidin was first immobilized on a sensor CM-5 chip via a primary amine chemical coupling reaction. A continuous flow of HBS was maintained at 5 μL/min. The chip surface was activated by injection of 50 μL of a mixture of 50 mM EDC and 50 mM NHS. Then 50 μL of streptavidin (0.2 mg/mL in 10 mM sodium acetate, pH 4.5) was injected, followed by injection of 40 μL of 1.0 M ethanolamine hydrochloride (pH 8.0) to block the remaining activated carboxyl groups. Loosely bound streptavidin was washed away by injection of 10 μL of 0.05% (w/v) SDS. Usually, approximately 5000 resonance units or response units (RU) of streptavidin were immobilized. The biotin-labeled single-stranded oligonucleotides were then injected manually until the required response units were observed (typically 100 RU from 5 μL of 0.5 μg/mL DNA in HBS buffer). This was followed by the injection of an excess of the complementary strand of DNA (typically 20 μL of 2 μg/mL DNA in HBS) until there was no increase of RU. Usually 150−200 RU of DNA was immobilized on each flow cell for kinetic analysis. When a sensor SA chip (with preimmobilized streptavidin) was used, the above steps for the immobilization of streptavidin were omitted, and the biotin-labeled DNA was immobilized directly on the chip. Finally, 20 μL of 80 μg/mL biotin in HBS was injected, to block the remaining biotin binding sites on the streptavidin and reduce possible nonspecific binding.

Kinetic Analysis and Efficiency of IN Binding to DNA Substrates. For the BIAcore experiments, enzyme was taken from storage and diluted to twice its volume with 10 mM HEPES (pH 7.5), containing 300 mM KCl, 1 mM DTT, 0.5 mM EDTA, and 0.005% surfactant P20 (buffer A), followed by dialysis in 1000 mL of the same buffer. 300 mM KCl in buffer A was used to suppress both nonspecific interaction of IN with chip surfaces and catalytic reactions of IN which may change the sequences of DNA immobilized on the chip surface. After dialysis, the buffer was filtered through a 0.2 μm membrane, degassed with vacuum for 20 min, and then used as running buffer. After centrifugation of the dialyzed IN at 17000*g* for 10 min, protein concentrations of the supernatants were determined using the Bio-Rad protein assay reagent with bovine serum albumin as standard. BIAcore experiments were performed by injection of HIV-1 IN at various concentrations in a random order at a rate of 30 μL/min, except where specified, over a biosensor chip containing immobilized DNA. The bound proteins were stripped off by injection of 20 μL of 0.035% (w/v) SDS in HBS, and the chip surface was subsequently washed with an excess of buffer A after each cycle. The data were analyzed with the computer software Bioevaluation 3.0 (Pharmacia).

The kinetic rate constants for dissociation (k_{off} or k_d) and for the apparent association (k_{on} or k_a), leading to apparent dissociation constant ($K_d = k_{off}/k_{on}$), were obtained by fitting the real-time data separately. We observed a biphase dissociation in these analyses with a initial faster decay lasting ~20 s, followed by a slower decay. Because a decay similar to the faster dissociation was observed when IN protein was immobilized on a chip, it is likely that the initial decay includes the dissociation of multimeric IN forms. Thus, to isolate the effects of IN−DNA interactions, rate constants were determined by fitting dissociation phases from 30 to 180 s. These rates are independent of IN concentrations, and the k_{off} values obtained reflect mainly the dissociation of IN from the immobilized DNA. On the other hand, association rate constants are dependent on protein concentration. Absolute values for these constants could not be obtained because the HIV-1 IN protein is a heterogeneous mixture in solution containing monomeric, dimeric, and even higher oligomeric forms (*4*, *10*, *36*, *45*, *50*). The relative proportions of each form may depend on the concentration of protein, the ionic strength, and the presence of metal cations. Furthermore, the presence of DNA may also affect these proportions. As it was not possible to quantify the effects of all of these variables, for the sake of comparison, we calculated *apparent* association rate constants by expressing protein concentration in terms of a dimer, which is reported to be the dominant form in HIV−IN preparations (*36*, *45*, *47*, *50*), and by assuming that at relatively low IN concentra-

tions one IN dimer is bound to one DNA substrate molecule in a model reaction:

$$\text{DNA} + (\text{IN})_2 \underset{k_{\text{off}}}{\overset{k_{\text{on}}}{\rightleftharpoons}} \text{DNA}\cdot(\text{IN})_2 \qquad \text{(reaction 1)}$$

The association rate constants were subsequently fit to association phases of the real-time data and k_{off} values obtained. To compare the kinetic parameters of IN binding to a DNA substrate in the presence of Me^{2+} with those in the absence of Me^{2+} (0.5 mM EDTA), we performed the experiments at the same enzyme concentrations and buffer conditions. A concentration of 7.5 mM Me^{2+} was used as this is within the range of optimal concentrations determined for IN activity in vitro (*36*). Both the IN protein preparation and running buffer included the indicated divalent cations. When reaction 1 reached equilibrium, a kinetic analysis was also performed using a Lineweaver−Burk plot with

$$\frac{1}{\text{RU}} = \frac{K_{\text{d}}}{a}\cdot\frac{1}{[\text{IN}]} + \frac{1}{a} \qquad \text{(eq 1)}$$

Relative resonance units (RU) are directly proportional to the surface concentrations of IN−DNA complexes. In all cases, the K_{d} values estimated from the Lineweaver−Burk plots were ~10-fold higher than those obtained by fitting the real-time data, suggesting that the IN−DNA interaction may need a higher oligomeric form of IN.

To measure the efficiency of IN binding to the DNA substrates, 105 μL of IN (at 20−2000 nM) was injected. The observed RU values, representing the binding efficiency, were represented in a plot of 1/RU vs 1/[IN]. The results obtained in the absence of a divalent cofactor were compared with the results in the presence of a divalent cofactor.

RESULTS

The HIV-1 IN-3CS Enzyme Exhibits Wild-Type Activity in Vitro. Our initial attempts to study HIV-1 IN−DNA interactions using surface plasmon resonance (SPR) were not successful owing to the low solubility of the wild-type protein under our assay conditions and the strong, nonspecific interactions between a chip and IN F185K, C280S, a soluble variant protein characterized previously (*50*). We had observed that addition of the reducing agent, DTT, to our protein preparations increased the concentration of soluble integrase recovered from our purification. Hypothesizing that the low solubility was due, in part, to formation of intermolecular disulfide bonds, we mutated our expression plasmid such that all of the cysteine codons (Cys 56, 65, 130, and 280 in Figure 1A) outside of the HHCC domain were changed to serine codons. Because Cys 40 and 43 (in the HHCC domain) coordinate a zinc ion that stabilizes the structure of the N-terminal domain, these cysteine residues were not changed (*7*, *8*, *49*). Singly-, doubly-, triply-, and quadruply-substituted cysteine to serine derivatives of HIV-1 IN protein were prepared and analyzed. We found that HIV-1 IN C56S, C65S, C280S (HIV-1 IN-3CS) was the most soluble derivative. Whereas wild-type HIV-1 IN is soluble to ~1 mg/mL, HIV-1 IN-3CS is soluble to about 15 mg/mL under identical conditions. Size-exclusion chromatography showed that unlike the soluble F185K, C280S derivative of HIV-1 IN that is primarily dimeric (at 1−10 μM concentrations) (*45*, *50*), HIV-1 IN-3CS behaves like the wild-type protein (*47*) and consists of comparable mixtures of monomers, dimers, and higher-order oligomers at equivalent concentrations (data not shown). The soluble HIV-1 IN-3CS retains catalytic activity, and it is as active in vitro as the wild-type protein for both processing (Figure 1B) and joining reactions (not included). Our preliminary results indicate that the change of the three cysteines to serines does not impair replication of the mutant virus in tissue culture. Therefore, except where specified in Table 1(footnote *f*), IN-3CS was used for all of the experiments in this study.

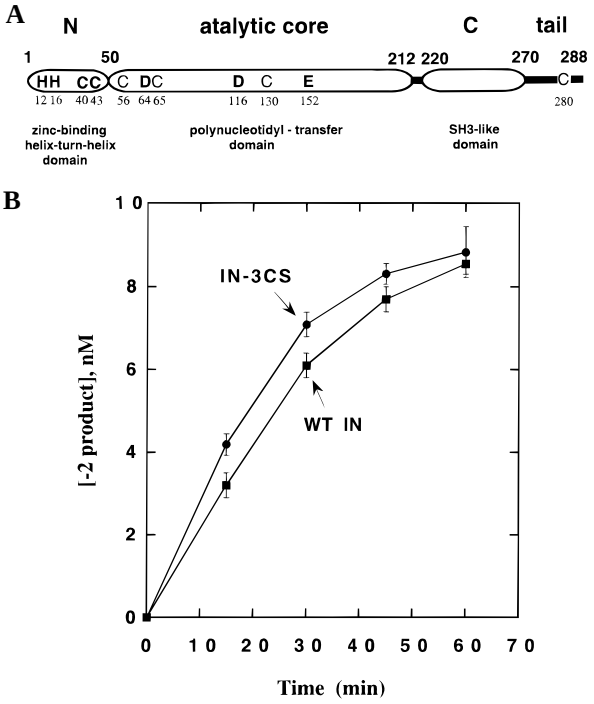

FIGURE 1: (A) A linear model of HIV-1 integrase protein showing the positions of critical residues and three functional domains as well as a C-terminal tail. The N-terminal domain with a helix−turn−helix structure contains the conserved residues HHCC and binds a zinc ion (*7*). The catalytic core domain, with polynucleotidyl-transfer activity, has a highly conserved D,D(35)E motif and binds Mg^{2+} (*15*, *16*). The C-terminal domain with a SH3-like structure (*49*, *66*) has a nonspecific DNA binding activity. The numbers above the map indicate the approximate borders of the domains, and numbers below the map show the positions of the conserved residues of HIV-1 IN. The positions of four cysteine residues (56, 65, and 130 in the core domain, and 280 at the tail), which were substituted with serines in this study, are also indicated. (B) Processing activities of wild-type HIV-1 IN and HIV-1 IN-3CS. The processing activities of wild-type HIV-1 IN (■) and IN-3CS (●) were followed over 60 min. The reaction mixtures contained 1 μM ^{32}P-labeled 21 bp model viral DNA substrate, 1 μM IN protein in 25 μL of 20 mM Hepes buffer (pH 7.5), 10 mM $MnCl_2$, 6.67% Me_2SO, 10% glycerol, and 50 mM KCl. Every 15 min, 5 μL aliquots were removed and quenched with an equal volume of loading buffer. The samples were then subjected to electrophoresis on a 20% denaturing polyacrylamide gel containing 7 M urea. Processing was measured by quantitation of the −2 cleavage product, after exposure of the radioactive gel to an imaging plate and analysis on a Fuji MacBAS 2000 imaging system.

Formation of a Stable Complex of HIV-1 IN with Nonviral DNA in the Absence of Divalent Cations. Surface plasmon resonance was used to investigate the details of IN−DNA complex formation. In these experiments, solutions of IN were passed over the surface of a biosensor chip that contained immobilized duplex oligonucleotides as described

Table 1: Kinetic Parameters of HIV-1 IN Binding to DNA Substrates[a]

substrate[b]	KCl[c] (mM)	metal cofactor[d] (mM)	k_{on} ($\times 10^5$ M^{-1} s^{-1})	k_{off} ($\times 10^{-3}$ s^{-1})	K_d[e] (nM)
		(A) Model Target DNA			
24 bp DNA	300	(−)	1.3 ± 0.2	2.2 ± 0.3	17.0 ± 1.5
	300	Mg^{2+}: 10	0.9 ± 0.1	2.1 ± 0.2	23.0 ± 2.0
	300	Mn^{2+}: 7.5	0.4 ± 0.1	2.2 ± 0.1	53.0 ± 2.1
40 bp DNA	300	(−)	2.1 ± 0.5	2.3 ± 0.4	10.7 ± 1.0
	300	Mg^{2+}: 10	1.2 ± 0.2	1.4 ± 0.2	11.8 ± 1.0
		(B) Model Viral DNA			
21 bp blunt viral DNA end	300	(−)	0.7 ± 0.1	1.8 ± 0.4	27.6 ± 2.0
	300	Ca^{2+}: 7.5	0.8 ± 0.1	1.9 ± 0.3	24.0 ± 1.4
	300	Mg^{2+}: 7.5	2.2 ± 0.5	1.8 ± 0.1	7.9 ± 1.0
	300	Mg^{2+}: 10	2.0 ± 0.5	1.4 ± 0.3	7.1 ± 1.0
	300	Mn^{2+}: 7.5	1.0 ± 0.1	0.5 ± 0.1	4.6 ± 0.8
	150	(−)	6.9 ± 1.0	3.8 ± 0.2	5.5 ± 0.2[f]
	150	Mg^{2+}: 5	3.4 ± 1.0	0.4 ± 0.1	1.3 ± 0.1[f]
preprocessed 21 bp viral DNA end	300	(−)	1.7 ± 0.5	2.7 ± 0.1	16.4 ± 0.6
	300	Mg^{2+}: 7.5	1.5 ± 0.5	1.9 ± 0.2	12.5 ± 0.7
	300	Mn^{2+}: 7.5	1.5 ± 0.5	1.9 ± 0.1	12.6 ± 0.6
		(C) Mutated Viral DNA			
21 bp viral DNA end CA/GT→GT/CA	300	(−)	1.4 ± 0.4	2.2 ± 0.1	16.0 ± 0.5
	300	Mg^{2+}: 7.5	1.5 ± 0.3	2.3 ± 0.1	16.0 ± 0.5
	300	Mn^{2+}: 7.5	1.5 ± 0.4	2.1 ± 0.2	14.7 ± 0.6
33 bp extended viral DNA end	300	(−)	4.4 ± 0.5	1.5 ± 0.3	3.5 ± 0.3
	300	Mg^{2+}: 7.5	3.1 ± 0.5	1.6 ± 0.3	4.9 ± 0.4
	300	Mn^{2+}: 7.5	2.1 ± 0.4	1.2 ± 0.2	5.9 ± 0.5

[a] The BIAcore data were collected after passing IN protein over immobilized (100−200 RU) DNA substrate at 37 °C. Three to five different IN concentrations, equivalent to from 20 to 160 nM dimers, were used for each kinetic analysis. At these relatively low concentrations, it was assumed that the IN protein is primarily in dimer form, and concentrations were determined from the total IN concentrations (mg/mL) and IN dimer formula weight (64 kDa). Kinetic parameters were obtained by fitting real-time data to a one IN dimer to one DNA molecule interaction model. The *off* rates (k_{off}) were first determined by fitting the dissociation phases from 30−180 s after injections. The apparent *on* rate constants (k_{on}) were determined by fitting the association phases with the obtained *off* rate constants and the calculated IN dimer concentration (see Experimental Procedures). [b] The sequences of DNA substrates are listed under Experimental Procedures. [c] Indicated are the concentrations of salt (KCl) in enzyme buffers and flow through. [d] No divalent cation [labeled with (−)] was achieved by including 0.5 mM EDTA in both buffers for IN protein and for the flow through. [e] The dissociation constant was calculated from the ratio of the average of the *off* and the apparent *on* rates ($K_d = k_{off}/k_{on}$). The error was the maximum difference between the indicated value and the individual K_d value from each measurement. [f] These experiments were performed at 25 °C with wild-type HIV-1 protein.

under Experimental Procedures. The association and dissociation of IN and this DNA was monitored by the change in response units which are proportional to the surface concentration of bound analyte (*43*).

To investigate the stability of the nucleoprotein complex formed by IN with a model target DNA, a duplex 24 bp oligonucleotide with no sequence match with viral DNA ends was immobilized on a biosensor chip. Formation of the IN−DNA complexes was achieved by injection of 40 μL of 0.55 μM IN in buffer A with a flow rate of 25 μL/min (Figure 2A). To these complexes 5 μL of HBS buffer containing high concentrations of either NaCl (0.5−4 M), or methanol [10−75% (v/v)], or both 2.0 M NaCl and 50% methanol (Figure 2A) was injected as a pulse. The results showed no significant change in response units after the IN−DNA complexes were exposed to these conditions, indicating that the complex is highly stable to high ionic strength and hydrophobic solutions. Figure 2B shows the effects of increasing concentrations of SDS [0.005−0.04% (w/v)] on the stability of the IN−DNA complexes. We observed some dissociation with the lowest concentration and complete dissociation, with a return of response units to the base line, with 0.04% (w/v) SDS. This result suggests that structural features of IN are critical for the high stability of these IN−target DNA complexes.

Because duplex oligonucleotides with sequence corresponding to a viral end can also function as a target for DNA integration in vitro, HIV-1 IN should be able to form a stable complex with such DNA under the same conditions. As expected, when a 21 bp oligonucleotide representing the HIV-1 U5 viral DNA end was immobilized on the surface of a chip, results similar to those obtained with the nonviral DNA were observed (data not shown). Our results are consistent with previous reports (*3*, *36*) suggesting that a divalent metal cofactor is not absolutely necessary for stability of IN−DNA complexes. These results also imply that the model viral DNA binds to IN like a target DNA when a metal cofactor is not present.

Binding of IN to the Model Target DNA Substrate Is Reduced in the Presence of Mn^{2+}. Divalent metal ions, Mn^{2+} or Mg^{2+}, are required for retroviral integrase to catalyze integration reactions. Binding of these divalent metal cofactors induces a conformational change and activates HIV-1 IN (*45*, *51*). To determine if the presence of a divalent cation can influence the binding of IN to a model target DNA substrate, 105 μL of solutions containing increasing IN concentrations (equivalent to 20−2000 nM IN monomer, in buffer A) was injected in a random order over the surface of immobilized target DNA in the absence or in the presence of 7.5 mM Mn^{2+}. The relative response units were observed to increase with increasing IN concentration in both the absence and presence of Mn^{2+} (Figure 3A,B), demonstrating that the protein is soluble and functional for DNA binding under the conditions of the analyses. The relative response

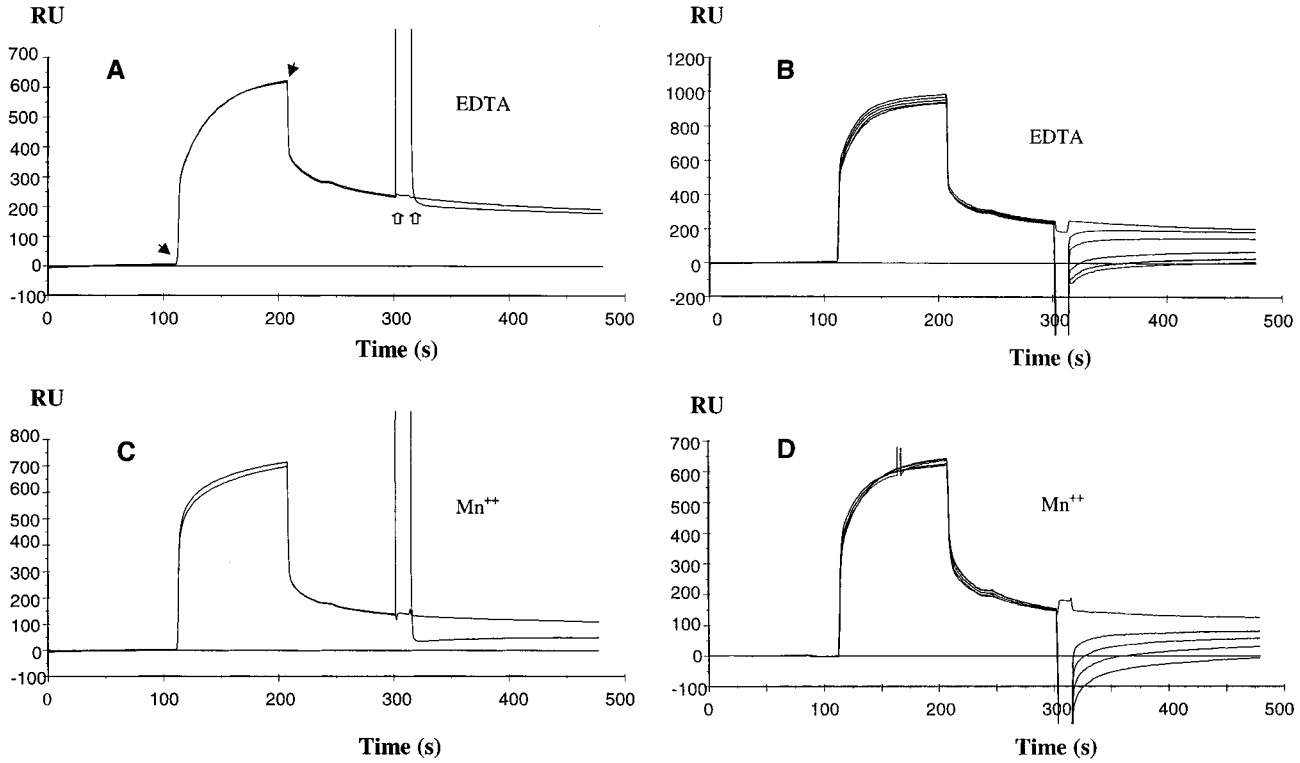

FIGURE 2: Stability of nucleoprotein complexes formed by HIV-1 IN with a model target DNA substrate. The biosensor surface contained 356 RU of immobilized 24 bp oligonucleotides representing a model target DNA substrate. 40 μL of 0.45 μM IN protein in buffer A in the absence of divalent cations or in the presence of 7.5 mM Mn^{2+} (C and D) was injected at a flow rate of 25 μL/min and 25 °C. Closed arrows in panel A indicate the beginning and end of this injection. The assembled IN−DNA complexes were then challenged by injection of either 5 μL of buffer A containing 2.0 M NaCl and 50% (v/v) MeOH (A and C) or 5 μL of HBS buffer containing SDS (B and D) as indicated by the open arrows in panel A. The expected base line, with no injection, is set as 0 in each panel. The challenging buffers from the top to bottom curves are as follows: (A) = buffer A with 2.0 M NaCl and 50% (v/v) MeOH; (B) = same as in (A) plus 0, 0.005, 0.01, 0.02, 0.03, 0.04% (w/v) SDS in HBS buffer; (C) = same as in (A) but with addition of 7.5 mM Mn^{2+}; (D) = same as in (A) plus 0, 0.005, 0.01, 0.02, 0.03% (w/v) SDS in HBS buffer, with addition of 7.5 mM Mn^{2+}.

units determined at 331.5 s, which excludes the bulk reflection upon injection, represent the relative binding efficiencies. The values obtained were replotted vs IN concentration as a double reciprocal (Figure 3C). These comparisons show that the binding of IN to the model target DNA was reduced in the presence of 7.5 mM Mn^{2+}. In the presence of 7.5 mM Mg^{2+}, reduced binding efficiency of HIV-1 IN to the model target DNA was observed only at low IN concentrations (Figure 3C), and the effect of this cation was less pronounced than that of Mn^{2+}. In each case, a hyperbolic-like curve was observed in the double-reciprocal plots (Figure 3C), suggesting that the HIV-1 IN−DNA interaction is a kinetically complicated process.

Kinetic parameters for association and dissociation were determined as described under Experimental Procedures at relatively low IN concentrations (calculated to be 20−160 nM IN dimer) to minimize the influence of possible aggregation and formation of higher-order IN multimers. When IN was injected at a concentration less than 10 nM (close to K_d; Table 1), no binding was detectable, suggesting that IN−DNA interaction requires a multimeric form of IN, most likely a dimer and higher oligomeric forms. The K_d value obtained for the IN−target DNA complex in the absence of divalent cofactor (17.0 nM in Table 1A) is consistent with the apparent high stability of the complex revealed by the results shown in Figure 2A. The K_d value increased to 53.0 and 23.0 nM in the presence of 7.5 mM Mn^{2+} and 10 mM Mg^{2+}, respectively, indicating that these divalent cofactors reduce the affinity of the IN−target DNA complex. These increases are consistent with the differences observed in Figure 2A,C where it is shown that the IN−DNA complex is significantly less stable after injection of 5 μL of 2.0 M NaCl and 50% (v/v) MeOH in the presence of 7.5 mM Mn^{2+} (Figure 2C) than it is under the same conditions in the absence of divalent cations (Figure 2A). The increases in K_d values are also consistent with the fact that the IN−DNA complex can be totally dissociated by injection of 5 μL of 0.03% (w/v) SDS in the presence of 7.5 mM Mn^{2+} (Figure 2D) compared to 0.04% (w/v) SDS in the absence of divalent cations (Figure 2B). The kinetic parameters summarized in Table 1A show that the increases in K_d values are due primarily to decreases in the *on* rate constants.

Divalent Cation Cofactors Stimulate the Binding of HIV-1 IN to the Model Viral DNA Substrate. Similar surface plasmon resonance experiments were performed with a duplex oligonucleotide representing the viral U5 DNA end. The effect of metal cofactors (Mg^{2+}, Mn^{2+}, or Ca^{2+}) on the interaction of IN with viral DNA was investigated by inclusion of either the divalent cation or 0.5 mM EDTA with the enzyme in the running buffer. Figure 4 shows the data expressed in double-reciprocal plots. In contrast to results with the target DNA (Figure 3C), the metal cofactors Mn^{2+} and Mg^{2+} were found to stimulate IN binding to the viral DNA substrate (Figure 4A,B). A much less pronounced stimulatory effect was observed with Ca^{2+} (Figure 4B). Kinetic calculations (Table 1B) show decreasing K_d values

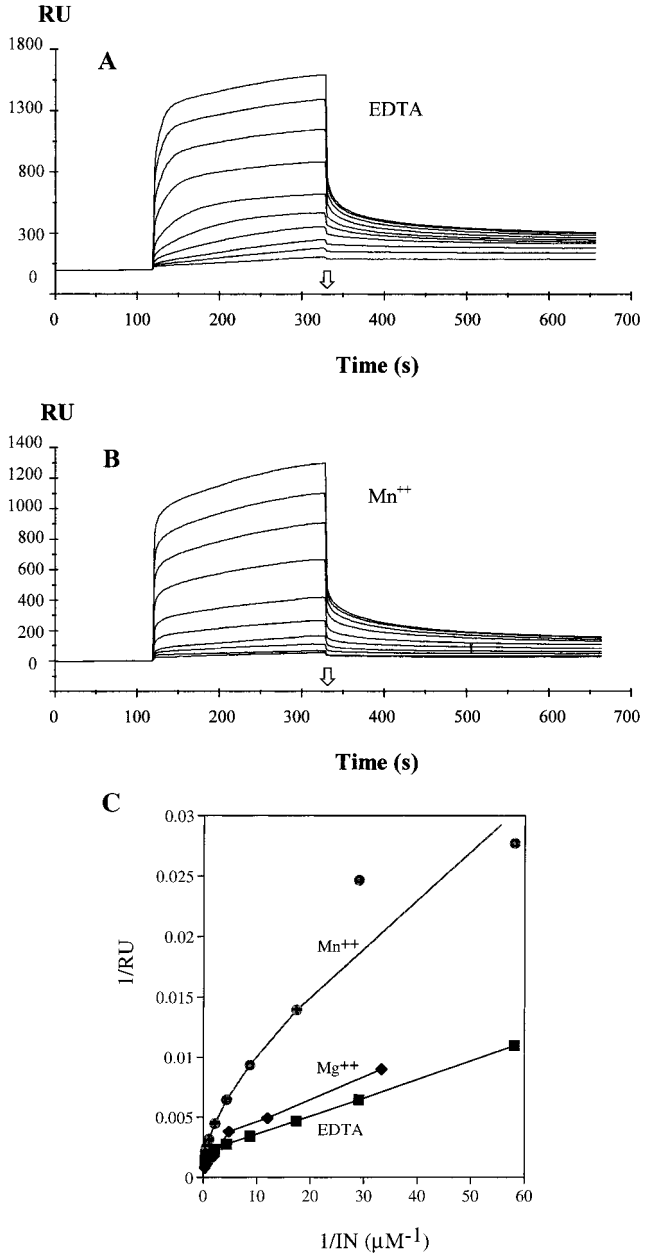

FIGURE 3: Effects of divalent cations on the binding efficiency of IN to a model target DNA substrate. (A) Overlay plot of IN binding to a model target DNA substrate in the absence of metal cofactors. To an immobilized (360 RU) target DNA substrate were injected 105 μL samples of IN protein (from 20 nM to 2.5 μM) in buffer A at 30 μL/min flow rate at 37 °C. (B) Overlay plots of IN binding to a model target DNA substrate in the presence of 7.5 mM Mn^{2+}. The experimental conditions were the same as in (A), but 7.5 mM Mn^{2+} was added both to the IN samples and to the running buffer. The base lines before the injections were adjusted to zero. (C) Effects of Mn^{2+} and Mg^{2+} on the dependence of IN binding efficiency as a function of the IN concentration. With elimination of bulk reflections due to the injection of IN solution, the relative response units at 331.5 s, as indicated by the open arrows in (A) and (B), were plotted vs IN concentrations as a double reciprocal: in the absence of divalent cations (■) and in the presence of 7.5 mM Mn^{2+} (●) or 7.5 mM Mg^{2+} (◆). The overlay plot of IN binding to the DNA substrate in the presence of Mg^{2+} is not shown, but the experiment was performed under the same conditions as indicated in (A), except for the addition of 7.5 mM Mg^{2+} in the enzyme and buffers.

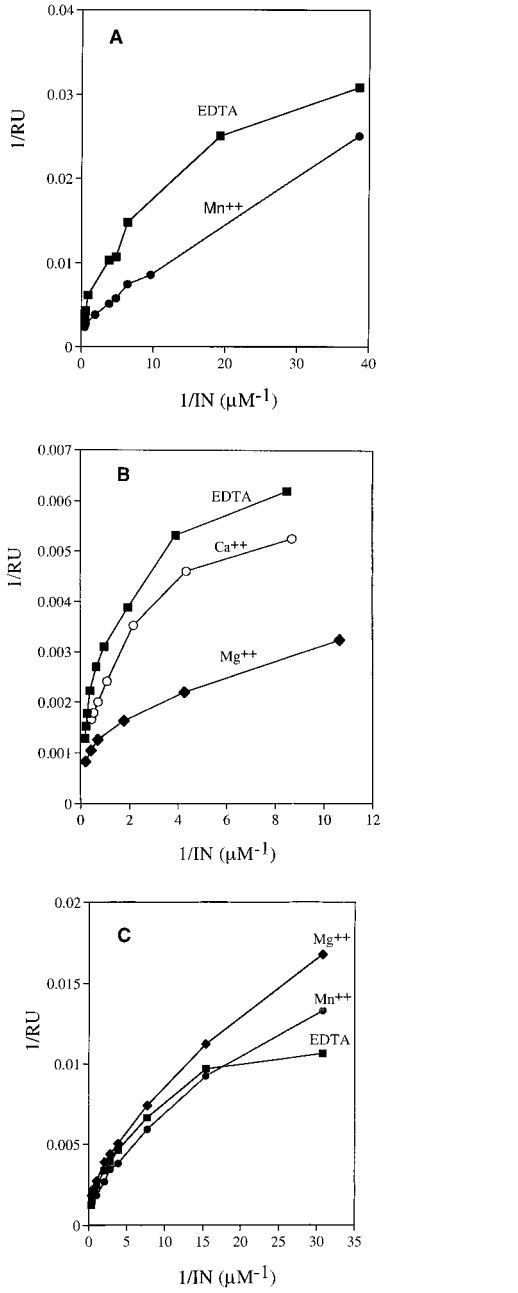

FIGURE 4: Stimulation by divalent metal cofactors of HIV-1 IN binding to model viral DNA end substrates. (A) Effect of Mn^{2+} on binding efficiency of IN to model viral blunt-ended DNA substrate expressed in a double-reciprocal plot. The experiments were carried out as described in the legend to Figure 3. 180 RU of 21 bp blunt-ended viral DNA end substrate was immobilized. The double-reciprocal plot shows the binding efficiency of IN at 37 °C in the absence of metal cofactors (■) or in the presence of 7.5 mM Mn^{2+} (●). (B) Effects of Mg^{2+} and Ca^{2+} on the binding efficiencies of IN to the viral DNA end substrate. Binding efficiency of IN was measured as described in (A) but with 532.5 RU of the immobilized DNA substrate. The plots show the dependence of IN binding efficiency on the IN concentration either in the absence of metal ions (■) or in the presence of 7.5 mM Mg^{2+} (◆) or 7.5 mM Ca^{2+} (○). (C) Effects of metal cofactors on the binding efficiency of IN to a preprocessed viral DNA end. 287 RU of 19/21 bp model preprocessed viral donor DNA substrate was immobilized. The binding efficiency of IN was measured either in the absence of metal cofactors (■) or in the presence of 7.5 mM Mn^{2+} (●) or 7.5 mM Mg^{2+} (◆). The experimental conditions were the same as described in the legend to Figure 3.

of 27.6, 24.0, 7.9, and 4.6 nM for no metal cofactor, 7.5 mM Ca^{2+}, 7.5 mM Mg^{2+}, and 7.5 mM Mn^{2+}, respectively.

These changes result from both an increase in the *on* rate constants and a decrease in the *off* rate constants in the

presence of metal cofactors (Table 1B). Thus, the affinity of IN for the viral DNA substrate is increased in the presence of metal ions, and the relative order of this effect is $Mn^{2+} > Mg^{2+} \gg Ca^{2+}$. This order is similar to that observed in a previous study which measured the ability of these cations to induce a conformational change in HIV-1 IN (*45*). The effects of the divalent cation cofactors on the efficiency of IN binding to DNA substrates suggest that the metal-induced conformational change allows HIV-1 IN to recognize and bind to the viral DNA end preferentially.

Divalent Cation Stimulation of IN Binding to Viral DNA Is Abolished by Alterations in the Viral DNA Sequence. As we observed that the effect of metal cofactors on HIV-1 IN binding to DNA substrates is DNA sequence-dependent, we next asked how changes in the viral DNA substrate might affect IN binding. The processing reaction produces a recessed viral DNA end resulting from the loss of two nucleotides from the 3′ end of the plus strand. The processed viral DNA is then a substrate for the next step in the reaction, joining to target DNA. To investigate the kinetics of interaction with processed viral DNA, binding assays were performed under the same conditions, but with a model "preprocessed" viral DNA substrate that contained a recessed 3′-OH end. The results showed that IN forms a stable complex with the preprocessed viral DNA, equally resistant to MeOH, NaCl, and SDS as the blunt-ended model viral DNA (data not included). This is consistent with a previous report that the viral DNA end remains bound to IN protein after the processing reaction (*34*). However, we observed little stimulation of binding activity by metal cofactors with the preprocessed viral DNA substrate (Figure 4C). Kinetic calculations show K_d values of 16.4, 12.5, and 12.6 nM in the absence of metal cofactor and in the presence of 7.5 mM Mg^{2+} or 7.5 mM Mn^{2+}, respectively (Table 1B). These values are 2−3 times higher than the K_d's calculated for blunt-ended viral DNA in the presence of the metal cofactors. This result suggests that the terminal dinucleotides that are absent in this preprocessed substrate may be important for the preferential recognition of blunt-ended viral DNA in the presence of divalent cations.

CA/TG base pairs are conserved near the ends of all retroviral DNAs. Mutation of these base pairs resulted in 10^5-fold reduction in integration of Moloney murine leukemia virus (MLV) DNA in vivo (*52*). Similar mutation of HIV-1 DNA substrates gave dramatic reduction of integration of HIV-1 DNA in vivo (*32*) and undetectable processing activity of HIV-1 IN in an in vitro assay (*24*, *53*, *54*). Thus, we asked if the CA/TG base pairs are required for the metal stimulation of IN binding to the viral DNA. We found that a blunt-ended viral DNA substrate in which these two base pairs were flipped showed no difference in the binding of IN in the absence or presence of Mg^{2+} or Mn^{2+} (Figure 5A). Kinetic calculations showed similar K_d values of 16.0, 16.0, and 14.7 nM in the absence of metal cofactor and in the presence of 7.5 mM Mg^{2+} or 7.5 mM Mn^{2+}, respectively (Table 1C). Thus, the stimulation of the binding activity of IN by the metal cofactors (Mg^{2+} or Mn^{2+}) was totally abolished by this mutation. These results indicate that the conserved CA/GT base pairs are also essential for the preferential recognition of viral DNA in the presence of the divalent cations.

Biochemical and genetic studies have shown that the specific viral DNA sequences that are recognized by IN need

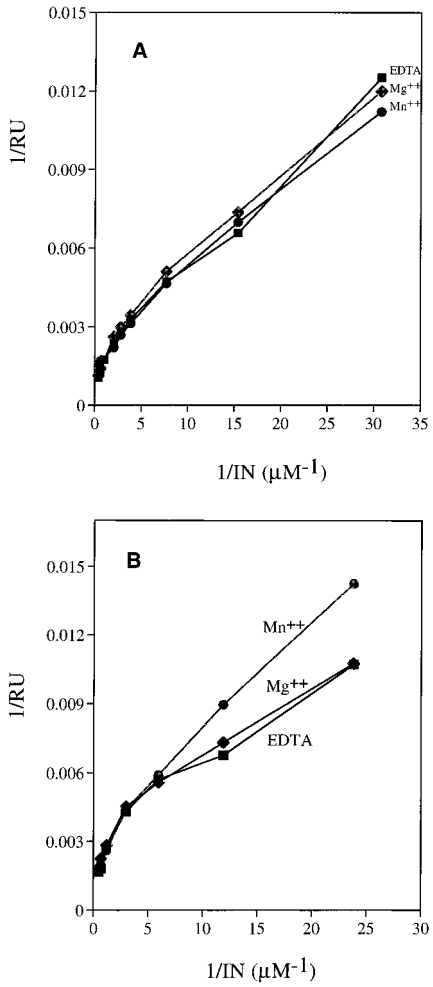

FIGURE 5: Effect of metal ions on the binding efficiency of HIV-1 IN to altered viral DNA ends. (A) The double-reciprocal plots show the dependence of the efficiency of IN binding to a 21 bp viral DNA end (138 RU) with a flipped CA/GT bp on the concentrations of IN, in the absence of metal cofactors (■) or in the presence of 7.5 mM Mn^{2+} (●) or 7.5 mM Mg^{2+} (◆). (B) Double-reciprocal plot showing binding efficiency of IN to a viral DNA end extended with 14 bp nonviral DNA (145 RU) in the absence of metal cofactors (■) or in the presence of 7.5 mM Mn^{2+} (●) or 7.5 mM Mg^{2+} (◆).

to be near the end of the DNA. Therefore, we constructed and tested a viral DNA substrate in which the normal end was extended by 14 base pairs of nonviral sequence. We found that in this case, as well, no cofactor stimulation of IN binding to the viral DNA substrate was observed. In fact, the binding efficiency in the presence of Mn^{2+} was actually somewhat lower than that in the absence of the metal cofactor (Figure 5B), similar to the situation with the model target DNA (Figure 3C). With the 35-mer extended viral DNA substrate, the K_d values were raised from 3.5 to 5.9 nM by the addition of 7.5 mM Mn^{2+}, and to 4.9 nM by the addition of 7.5 mM Mg^{2+} (Table 1C). These results suggest that a free viral DNA end is required for divalent cation stimulation of IN recognition by HIV-1 IN.

Affinity of IN−DNA Complexes Is Influenced by Salt and DNA Length. The kinetic parameters summarized in Table 1 show that in all cases the *off* rates are close to $(0.4-4.0) \times 10^{-3}$ s^{-1}, and the *on* rates are near $(0.4-7.0) \times 10^5$ M^{-1} s^{-1}, consistent with the interpretation that there is a lack of absolute binding specificity of HIV-1 IN to the substrates

(*36*, *38*). However, a combination of these two kinetic factors results in substantial differences in the apparent K_d values between viral DNA substrate and nonviral DNA substrate. It can be seen that the stabilities of IN−nonviral DNA complexes are increased with increasing length of DNA (Table 1A,C). This result is consistent with a previous report that the affinity of the IN−viral DNA complex increases with the length of viral DNA substrates (*55*). On the other hand, the affinities of IN−viral DNA complexes are decreased with increasing salt concentration (Table 1B). In the absence of any divalent metal, the apparent k_{on} values change from 6.9 $\times 10^5$ M^{-1}•s^{-1} in 150 mM KCl to 0.7 $\times 10^5$ M^{-1}•s^{-1} in 300 mM KCl. This change in the k_{on} values is a primary source of the increase in K_d values from 5.5 nM in 150 mM KCl to 27.6 nM in 300 mM KCl. The change may signify that the conformation of IN protein is affected by the salt concentration. In the presence of Mg^{2+}, the K_d value increases from 1.3 to 7.6 nM when KCl is increased from 150 to 300 mM, and both the decrease in the k_{on} values and the increase in the k_{off} values contribute to the increase in the K_d values.

DISCUSSION

HIV-1 IN forms highly stable complexes with either model viral DNA or model target DNA substrates. The complexes are resistant to challenge by either high salt concentration, high methanol, or both, but are not resistant to low concentration of SDS (Figure 2). These properties suggest that the structural features or the conformation of IN protein, rather than its charge, plays a major role in the IN−substrate interaction. Two DNA-sequence dependent effects of metal cofactors were observed with the IN−DNA interaction. With nonviral model target DNA substrates, Mn^{2+} decreased the binding efficiency of IN to the DNA substrate. Mg^{2+} also decreased this binding but with less effect than Mn^{2+} (Figure 3C). In contrast, with a model viral DNA substrate, both Mg^{2+} and Mn^{2+} stimulated binding of IN (Figure 4A,B), and stabilized the IN−viral DNA complexes.

In the absence of a divalent metal cofactor, IN bound to the 21 bp viral DNA substrate (apparent $K_d = 27.6$ nM at 300 mM KCl, Table 1B) with affinity similar to that observed for the 24 bp nonviral, target DNA substrate (17.0 nM, Table 1A). Thus, IN exhibits no preference for the viral DNA in the absence of the cofactors. In the presence of 7.5 mM Mg^{2+}, the dissociation constants are changed to 7.9 nM for viral DNA and 23.0 nM for the target DNA; the difference is even more pronounced in the presence of 7.5 mM Mn^{2+} with apparent K_d values of 4.6 and 53.0 nM for the viral and target DNAs, respectively (Table 1A,B), a greater than 11-fold difference. In standard in vitro assays, a 21 bp viral DNA end functions both as a viral DNA and as a target DNA substrate. Thus, our kinetic calculations with the model viral DNA substrate may reflect an average of both effects of the metal ion. The actual differences in the ability of the enzyme to recognize viral and target DNAs in the presence of Me^{2+} may be much greater. Furthermore, during concerted integration of two viral DNA ends into a target DNA in vitro, we can expect that the Me^{2+} effects will increase to the square of the results we observed with a single viral DNA end.

Transposition reactions catalyzed by transposases, such as the MuA transposase, are mechanistically similar to the retroviral integration reaction (*56*, *57*). Structural comparisons place these proteins and integrases in the same super-family (*58*), and they may share a similar mechanism of catalysis. Formation of stable MuA−Mu DNA end complexes is dependent on the presence of either Mg^{2+}, Mn^{2+}, or Ca^{2+} (*59*, *60*). In the assembly of HIV-1 IN−viral DNA complexes, both a stabilizing effect of Ca^{2+} on the complexes (*34*, *35*) and no significant effect of Ca^{2+} have been reported (*33*). In our experiments, 7.5 mM Ca^{2+} exhibited a minimal effect both on the stimulation of IN binding to viral DNA substrate (Figure 4B) and on the stability of the IN−viral DNA complexes revealed by kinetic analysis (Table 1B). This is consistent with our previous observations that a relatively high concentration of this cation was required to observe a conformational change in HIV-1 IN (*45*), and with a report that preincubation of IN with Ca^{2+} only slightly enhanced IN activity in vitro (*33*).

Our observed cofactor stimulation of the binding of IN to viral DNA and the resulting decreases in apparent K_d values are consistent with previous reports that the metal cofactors promoted formation of stable IN−viral DNA complexes (*33*, *34*). We found that these effects were abolished by the extension of the viral DNA end with nonviral sequences, or by substitution of the conserved CA/TG base pair with a GT/AC base pair (Figure 5A,B), and were diminished with a preprocessed model viral DNA end (Figure 4C). Ellison and Brown (*33*) reported that a 2 bp deletion from the 5′ end (AC) of HIV-1 DNA minus strand of U5 DNA also destabilized the IN−viral DNA complex. Taken together, these results suggest that the last 4 bp and a free viral DNA end are critical for the metal ion stimulation of IN binding to viral DNA, and for stabilization of the IN−viral DNA complexes. On the other hand, the effect of divalent cations on IN binding to the flipped CA/GT-altered viral DNA substrates (Figure 5A) is similar neither to the stimulation seen with the blunt model viral DNA substrate (Figure 4A,B) nor to the reduction observed with a model target DNA substrate (Figure 3C). Thus, other residues upstream from the viral DNA end may also contribute to IN recognition (*27*, *28*, *30*−*32*, *54*).

Our results show that at equal concentrations Mn^{2+} induces stronger effects than Mg^{2+} both on the enhancement of IN binding to the viral DNA substrate and on the reduction of IN binding to the target DNA substrate. These differences may explain why Mn^{2+} is generally more effective than Mg^{2+} as a cofactor for catalysis in the in vitro assay. In addition, Mn^{2+} is more effective at stabilizing the IN−viral DNA complexes than Mg^{2+}, which may be important for the processing reaction (*36*). Mn^{2+} may also be more effective than Mg^{2+} in inducing release of the DNA product after catalysis. The k_d (*off* rate constant) of IN bound to 33 bp extended viral DNA complexes at 50 mM KCl in the presence of 5 mM Mg^{2+} is $\sim 3 \times 10^{-4}$ s^{-1}, i.e., 0.018 min^{-1}. This is comparable to values of k_{cat} reported for the processing reaction of HIV-1 IN: 0.046 and 0.069 min^{-1} in the presence of 5 mM Mn^{2+} and Mg^{2+}, respectively (*36*), 0.0021 min^{-1} in the presence of 10 mM Mn^{2+} (*61*), and 0.004 min^{-1} in the presence of 7.5 mM Mg^{2+} (*62*). The k_{cat} of the joining reaction of integration is reported to be close to, but no greater than, that of the processing reaction (*63*). Thus, product release is, or contributes to, the rate-limiting step. Destabilization of the IN−product DNA complexes by Mn^{2+} could facilitate turnover by enhancing the release of product.

Alternatively, metal ions may help IN to bind to viral DNA in the right orientation, position, or conformation so that the catalytic reactions can be performed. It is also possible that the metal cofactor may shift the equilibria among multimeric forms of IN to favor IN−viral DNA interaction but not IN−target DNA interaction.

Stimulation of HIV-1 IN binding to viral DNA by metal cofactors was observed by Pemberton and co-workers (*36*). Their results were explained by a positive cooperative binding of IN to viral DNA substrates induced by metal cofactors. However, our data for the binding of IN to the model viral substrate (Figure 4A,B), to the viral DNA end extended with 14 bp of nonviral sequence (Figure 5B), and to the model target DNA substrate (Figure 3C) show that the plots of 1/RU vs 1/[IN] deviate from straight lines into hyperbolic-like curves. The pattern of these plots indicates that the affinity of IN−DNA complexes decreases with increasing IN concentration. This suggests that a negative cooperativity, if any, may exist between two IN molecules binding to one DNA substrate even in the presence of metal cofactors (*64*). This may signify that a DNA binding site is close to a protein−protein interface in multimeric forms of IN. However, the bending in the double-reciprocal plots may also result from more complicated interactions between HIV-1 IN and its substrates, such as specific IN protein−protein interactions and/or a DNA-induced protein conformation change. When the IN concentration is increased, the equilibrium shifts to favor higher multimeric IN forms. Owing to their higher mass, such multimeric forms (e.g., tetramers) could contribute disproportionately to an increase in RU even though they have the same DNA binding property as dimers. In fact, after IN was loaded onto the DNA, two dissociation phases were observed (Figure 3A,B) with an initial, fast dissociation ($k_{off} \sim 5 \times 10^{-2}$ s^{-1}) followed by a slower decay ($k_{off} \sim 1 \times 10^{-3}$ s^{-1}, Table 1). This suggests that two or more complexes of different stabilities were formed on the chip surface. The fraction of less stable complex (apparent $K_d \sim 1 \times 10^{-6}$ M) was higher at a higher IN concentration, as we observed that the initial, fast decay became more obvious at higher IN concentration (Figure 3A,B). Therefore, this faster decay may reflect the dissociation of IN either from a less stable complex with DNA or from other protein molecules in an IN−(IN−DNA) complex. Further experiments will be required to distinguish between these two possibilities. Furthermore, as both the initial fast decay ($k_{off} \sim 5 \times 10^{-2}$ s^{-1}) and the late slower decay ($k_{off} \sim 1 \times 10^{-3}$ s^{-1}) decreased slightly with increase in sample loading times at lower IN concentrations (data not shown), it is also possible that the DNA substrates induce a protein conformation change (*37*) that allows formation of a more stable nucleoprotein complex.

Significant progress in our understanding of IN−DNA interactions has been made in recent years. Both the catalytic core domain and the C-terminal domain of HIV-1 IN are known to contribute to nonspecific DNA binding (*40*). Photo-cross-linking studies indicate that viral DNA can bind to peptides in both the core and C-terminal domains, but target DNA can bind to peptides in all three domains (*65*). The minimum region of IN required for nonspecific DNA binding has been mapped to residues 220−270 in the C-terminal domain (*19*) whose structure has been solved (*49*, *66*). Mutagenesis studies have revealed that Lys 264, Arg 262, and Leu 234 in this domain contribute to DNA binding (*19*, *67*). Although the isolated core domain of HIV-1 IN shows no detectable binding to any linear DNA, even in the presence of metal ions (*40*; also our unpublished data), the core domain does harbor some or all of the determinants responsible for recognition of the CA/GT dinucleotides (*21*, *68*, *69*). In fact, the core domain can bind to a model branched DNA intermediate of integration, and recognize key features of the DNA substrate (*70*). A core region corresponding to residues 153−167 was identified as a nucleotide (5N3-AZTMP) binding site (*71*), and the residues Lys 136 (*72*), Lys 156, and Lys 159 (*73*) can be cross-linked to, or close to, the conserved CA dinucleotide in the viral DNA end. Mutagenesis studies also suggested that Gln148 may be involved in the binding of viral DNA ends (*74*). Recent molecular modeling studies suggest that at least eight IN protomers mediate the concerted integration of the two viral DNA ends into a target DNA (*75*). How such a nucleoprotein complex may be assembled is not understood. Our results suggest that the predominant forces for formation of highly stable IN−target DNA or IN−viral DNA complexes are the same in the absence of divalent cations. However, in the presence of the metal cofactor, IN can discriminate between viral and nonviral DNA, and the last 4 bp in the viral DNA ends are especially important for such discrimination.

ACKNOWLEDGMENTS

We acknowledge Drs. Michael Robinson and Sheree Long of BIAcore for their expert advice on the BIAcore technology. We express our gratitude to Dr. Robert Fisher at NCI−Frederick Cancer Research and Development Center, Frederick, MD, and Drs. Richard Katz, Mark Andrake, Anthony Yeung, Steven Seeholzer, and George Markham of the Fox Chase Cancer Center for their critical review of the manuscript and helpful discussions.

REFERENCES

1. Katz, R. A., and Skalka, A. M. (1994) *Annu. Rev. Biochem. 63*, 133−173.
2. Kukolj, G., and Skalka, A. M. (1995) *Genes Dev. 9*, 2556−2567.
3. Goodarzi, G., Im, G.-J., Brackmann, K., and Grandgenett, D. (1995) *J. Virol. 69*, 6090−6097.
4. Andrake, M. D., and Skalka, A. M. (1996) *J. Biol. Chem. 271*, 19633−19636.
5. McEuen, A. R., Edwards, B., Ball, A. E., Jennings, B. A., Wolstenholme, A. J., Danson, M. J., and Hough, D. W. (1992) *Biochem. Biophys. Res. Commun. 189*, 813−818.
6. Bushman, F. D., Engelman, A., Palmer, I., Wingfield, P., and Craigie, R. (1993) *Proc. Natl. Acad. Sci. U.S.A. 90*, 3428−3432.
7. Cai, M., Zheng, R., Caffrey, M., Craigie, R., Clore, G. M., and Groneborn, A. M. (1997) *Nat. Struct. Biol. 4*, 567−577.
8. Zheng, R., Jenkin, S. T. M., and Craigie, R. (1996) *Proc. Natl. Acad. Sci. U.S.A. 93*, 13659−13644.
9. Lee, S. P., and Han, M. K. (1996) *Biochemistry 35*, 3837−3844.
10. Lee, S. P., Xiao, J., Knutson, J. R., Lewis, M. S., and Han, M. K. (1997) *Biochemistry 36*, 173−180.
11. Khan, K., Mack, J. P. G., Katz, R. A., Kulkosky, J., and Skalka, A. M. (1990) *Nucleic Acids Res. 19*, 851−860.
12. Kulkosky, J., Jones, H. S., Katz, R. A., Mack, J. P. G., and Skalka, A. M. (1992) *Mol. Cell. Biol. 12*, 2331−2338.
13. Bujacz, G., Jaskolski, M., Alexandratos, J., Wlodawer, A., Merkel, G., Katz, R. A., and Skalka, A. M. (1995) *Structure (London) 4*, 89−96.

14. Bujacz, G., Alexandratos, J., Wlodawer, A., Merkel, G., Andrake, M., Katz, R. A., and Skalka, A. M. (1997) *J. Biol. Chem. 272*, 18161−18168.
15. Maignan, S., Guilloteau, J.-P., Zhou-Liu, Q., Clément-Mella, C., and Mikol, V. (1998) *J. Mol. Biol. 282*, 359−368.
16. Goldgur, Y., Dyda, F., Hickman, A. B., Jenkins, T. M., and Craigie, R. (1998) *Proc. Natl. Acad. Sci. U.S.A. 95*, 9150−9154.
17. Woerner, A. M., Klutch, M., Levin, J., and Marcus-Sekura, C. J. (1992) *AIDS Res. Hum. Retroviruses 8*, 297−304.
18. Vink, C., Oude, G. A. A. M., and Plasterk, R. H. A. (1993) *Nucleic Acids Res. 21*, 1419−1425.
19. Puras-Lutzke, R. A., Vink, C., and Plasterk, R. H. A. (1994) *Nucleic Acids Res. 22*, 4125−4131.
20. Misa, T. K., Grandgenett, D. P., and Parsons, J. T. (1982) *J. Virol. 44*, 330−343.
21. Kulkosky, J., Katz, R. A., Merkel, G., and Skalka, A. M. (1995) *Virology 206*, 448−456.
22. Krogstad, P. A., and Champoux, J. J. (1990) *J. Virol. 64*, 2796−2801.
23. Basu, S., and Varmus, H. E. (1990) *J. Virol. 64*, 5617−5625.
24. Sherman, P. A., and Fyfe, J. A. (1990) *Proc. Natl. Acad. Sci. U.S.A. 87*, 5119−5123.
25. Sherman, P. A., Dickson, M. L., and Fyfe, J. A. (1992) *J. Virol. 66*, 3593−3601.
26. LaFemina, R. L., Callahan, P. L., and Cordingley, M. G. (1991) *J. Virol. 65*, 5624−5630.
27. Vink, C., van Gent, D. C., Elgersma, Y., and Plasterk, R. H. A. (1991) *J. Virol. 65*, 4636−4644.
28. Leavitt, A. D., Rose, R. B., and Varmus, H. E. (1992) *J. Virol. 66*, 2359−2368.
29. Chow, S. A., and Brown, P. O. (1994) *J. Virol. 68*, 3896−3907.
30. Katzman, M., and Sudol, M. (1996) *J. Virol. 70*, 9069−9073.
31. Balakrishnan, M., and Jonsson, C. B. (1997) *J. Virol. 71*, 1025−1035.
32. Masuda, T., Kuroda, M. J., and Harada, S. (1998) *J. Virol. 72*, 8396−8402.
33. Vink, C., Puras-Lutzke, R. A., and Plasterk, R. H. A. (1994) *Nucleic Acids Res. 22*, 4103−4110.
34. Ellison, V., and Brown, P. O. (1994) *Proc. Natl. Acad. Sci. U.S.A. 91*, 7316−7320.
35. Hazuda, D. J., Jelock, P. J., Hastings, J. C., Pramanik, B., and Wolfe, A. L. (1997) *J. Virol. 71*, 7005−7011.
36. Pemberton, I. K., Buckle, M., and Buc, H. (1996) *J. Biol. Chem. 271*, 1498−1506.
37. Pemberton, I. K., Buc, H., and Buckle, M. (1998) *Biochemistry 37*, 2682−2690.
38. van Gent, D. C. V., Elgersma, Y., Bolk, M. W. J., Vink, C., and Plasterk, R. H. A. (1991) *Nucleic Acids Res. 19*, 3821−3827.
39. Hazuda, D. J., Wolfe, A. L., Hastings, J. C., Robbins, H. L., Graham, P. L., LaFemina, R. L., and Emini, E. A. (1994) *J. Biol. Chem. 269*, 3999−4004.
40. Engelman, A., Hickman, A. B., and Craigie, R. (1994) *J. Virol. 68*, 5911−5917.
41. Yoshinaga, T., Kimura-Ohtani, Y., and Fujiwara, T. (1994) *J. Virol. 68*, 5690−5697.
42. Schauer, M., and Billich, A. (1992) *Biochem. Biophys. Res. Commun. 185*, 874−880.
43. Fisher, R. J., Fivash, M., Casas-Finet, J., Bladen, S., and McNitt, K. L. (1994) *Methods 8*, 121−133.
44. Myszka, D. G. (1997) *Curr. Opin. Biotechnol. 8*, 50−57.
45. Asante-Appiah, E., and Skalka, A. M. (1997) *J. Biol. Chem. 272*, 16196−16205.
46. Ausubel, F. M., Brent, R., Kingston, R. E., Moore, D. D., Seidman, J. G., Smith, J. A., and Struhl, K. (1998) *Short Protocols in Molecular Biology*, 2nd ed., pp 8.3−8.5, Green Publishing Associates/John Wiley & Sons, Inc., New York.
47. Asante-Appiah, E., Merkel, G., and Skalka, A. M. (1998) *Protein Expression Purif. 12*, 105−110.
48. Bonderson, Å., Fågertam, L., and Magnusson, G. (1993) *Anal. Biochem. 214*, 245−251.
49. Eijkelenboom, A. P. A. M., Puras-Lutzke, R. A., Boelens, R., Plasterk, R. H. A., Kaptein, R., and Hård, K. (1995) *Nat. Struct. Biol. 2*, 807−810.
50. Jenkins, T. M., Engelman, A., and Craigie, R. (1996) *J. Biol. Chem. 271*, 7712.
51. Asante-Appiah, E., Seeholzer, S., and Skalka, A. M. (1998) *J. Biol. Chem. 273*, 35078−35087.
52. Roth, M. J., Schwartzberg, P. L., and Goff, S. P. (1989) *Cell 58*, 47−54.
53. Bushman, F. D., and Craigie, R. (1991) *Proc. Natl. Acad. Sci. U.S.A. 88*, 1339−1343.
54. van den Ent, F. M. I., Vink, C., and Plasterk, R. H. A. (1994) *J. Virol. 68*, 7825−7832.
55. Lee, S. P., Censullo, M. L., Kim, H. G., and Han, M. K. (1995) *Biochemistry 34*, 10215−10223.
56. Engelman, A., Mizuuchi, K., and Craigie, R. (1991) *Cell 67*, 1211−1221.
57. Mizuuchi, K., and Adzuma, K. (1991) *Cell 66*, 129−140.
58. Rice, P., Craigie, R., and Davies, D. R. (1996) *Curr. Opin. Struct. Biol. 6*, 76−83.
59. Mizuuchi, M., Baker, T., and Mizuuchi, K. (1992) *Cell 70*, 303−311.
60. Baker, T., and Mizuuchi, K. (1992) *Gene Dev. 6*, 139−156.
61. Tramontano, E., Colla, P. L., and Chen, Y.-C. (1998) *Biochemistry 37*, 7237−7243.
62. Lee, S. P., Kim, H. G., Censullo, M. L., and Han, M. K. (1995) *Biochemistry 34*, 10205−10214.
63. Vincent, K. A., Ellison, V., Chow, S. A., and Brown, P. O. (1993) *J. Virol. 67*, 425−437.
64. Segel, I. H. (1975) *Enzyme Kinetics*, pp 346−385, Wiley-Interscience, London.
65. Heuer, T. S., and Brown, P. O. (1997) *Biochemistry 36*, 10655−10665.
66. Lodi, P. J., Ernst, J. A., Kuszewski, J., Hickman, A. B., Engelman, A., Craigie, R., Clore, G. M., and Gronenborn, A. M. (1995) *Biochemistry 34*, 9826−9833.
67. Puras-Lutzke, R. A., and Plasterk, R. H. A. (1998) *J. Virol. 72*, 4841−4848.
68. Katzman, M., and Sudol, M. (1998) *J. Virol. 72*, 1744−1753.
69. Shibagaki, Y., and Chow, S. A. (1997) *J. Biol. Chem. 272*, 8361−8369.
70. Gerton, J. L., and Brown, P. O. (1997) *J. Biol. Chem. 269*, 29279−29287.
71. Drake, R. R., Neamati, N., Hong, H., Pilon, A. A., Sunthankar, P., Hume, S. D., Milne, G. W. A., and Pommier, Y. (1998) *Proc. Natl. Acad. Sci. U.S.A. 95*, 4170−4175.
72. Mazumder, A., Neamati, N., Pilon, A. A., Sunder, S., and Pommier, Y. (1996) *J. Biol. Chem. 271*, 27330−27338.
73. Jenkins, T. M., Esposito, D., Engelman, A., and Craigie, R. (1997) *EMBO J. 16*, 6849−6859.
74. Gerton, J. L., Ohgi, S., Olsen, M., Derisi, J., and Brown, P. O. (1998) *J. Virol. 72*, 5046−5055.
75. Heuer, T. S., and Brown, P. O. (1998) *Biochemistry 37*, 6667−6678.

BI982870N